J. Chem. Sci., Vol. 118, No. 6, November 2006, pp. 525–536. © Indian Academy of Sciences.

The use of hydrothermal methods in the synthesis of novel open-framework materials

SRINIVASAN NATARAJAN*, SUKHENDU MANDAL, PARTHA MAHATA, VANDAVASI KOTESWARA RAO, PADMINI RAMASWAMY, ABHISHEK BANERJEE, AVIJIT KUMAR PAUL and K V RAMYA

Framework Solids Laboratory, Solid State and Structural Chemistry Unit, Indian Institute of Science, Bangalore 560 012
e-mail: snatarajan@sscu.iisc.ernet.in

Abstract. The preparation of inorganic compounds, exhibiting open-framework structures, by hydrothermal methods has been presented. To illustrate the efficacy of this approach, few select examples encompassing a wide variety and diversity in the structures have been provided. In all the cases, good quality single crystals were obtained, which were used for the elucidation of the structure. In the first example, simple inorganic network compounds based on phosphite and arsenate are described. In the second example, inorganic–organic hybrid compounds involving phosphite/arsenate along with oxalate units are presented. In the third example, new coordination polymers with interesting structures are given. The examples presented are representative of the type and variety of compounds one can prepare by careful choice of the reaction conditions.

Keywords. Hydrothermal methods; open-framework; single crystal XRD.

1. Introduction

The synthesis and study of novel inorganic compounds, especially those with specific functional groups, constitute an important area of research. A large number of synthetic approaches involving both mild as well as extreme conditions have been employed for the preparation of such compounds. Of these, compounds possessing extended network structures are an important class. In recent years, solids possessing extended structures have been attracting attention for their many applications in the area of catalysis, sorption and separation processes, both actual as well as potential. Many of these compounds have been prepared employing hydrothermal methods.

The term hydrothermal is purely of geological origin, which generally refers to any heterogeneous reaction in the presence of aqueous solvents or mineralisers under high pressure and temperature conditions to dissolve and recrystallise materials that are relatively insoluble under ordinary conditions. Sir Roderick Murchison (1792–1871), the British Geologist, used this term to describe the action of water at elevated temperature and pressure in bringing about the changes in the earth's crust leading to the formation of various minerals. The first successful commercial application of the hydrothermal method began with the mineral extraction or ore beneficiation during the 19th Century. Karl Josef Bayer (1871–1908) used sodium hydroxide to leach bauxite in 1892 as a process for obtaining pure aluminum hydroxide, under hydrothermal conditions. Further importance of the hydrothermal technique for the synthesis of inorganic compounds in a commercial way was realized soon after the synthesis of large single crystals of quartz and later aluminosilicate zeolites by Barrer.[1,2] The versatility of the hydrothermal procedure, mainly due to the mineralizing role of water, is quite apparent as it forms many minerals with considerable structural variety. Open aluminosilicate zeolite frameworks are stabilized during growth by being filled with guest molecules and hydrothermal method provides a facile route.

One of the important aspects of the hydrothermal method is to get the reactants, which are otherwise difficult to dissolve, into solution under the action of mineralisers or solvents. This is similar to the chemical transport reactions, which prompted definition of hydrothermal reactions as a special case of chemical transport reactions. Many of the fundamental physical properties of water like fugacity, dielectric constant, density etc. undergo considerable changes during the

*For correspondence

hydrothermal reaction at elevated temperatures. This has resulted in using this method for many types of reactions. Though traditionally hydrothermal method has been employed for the growth of large single crystals (quartz) and also for the leaching of ores during metal extraction, recent research has clearly shown that it is also highly beneficial for the preparation of new types of solids, especially complexes, coordination polymers[3] and microporous materials.[4]

Hydrothermal crystallizations are multi-component heterogeneous reactions involving several processes including equilibrium reactions, nucleation and growth. In many of the preparations of microporous solids under hydrothermal conditions, an organic amine molecule is used. The role of the organic amine molecule in the synthesis of such solids can be classified into three types: templating, structure-directing and space-filling. Here 'templating' refers to the formation of a unique structure, which reflects the geometrical and electronic structure of the template. Structure-direction describes the process where a specific organic amine preferentially leads to the synthesis of a structure by suitably influencing factors such as pH, solubility and electrostatic interactions. Space-filling is a process in which the organic amine excludes water and enhances the interactions in the organic-framework composite and thereby increases the thermodynamic stability.

During the synthesis of porous solids, irrespective of the role of the amine molecules, the amine molecules are, in general, located in cavities or channels and appears to direct the formation of a particular structure. The amine molecules can be removed by calcination, acid-leaching etc. to give a solid with large porous structure. Such solids are useful in the areas of catalysis, sorption and separation processes.

We have been employing the hydrothermal methods extensively for the past few years. The intense research activity resulted in many new compounds possessing a variety of structures. The compounds have zero-, one-, two- and three-dimensionally extended structures. The lower dimensional structures appear to be precursors for the formation of the structures of higher dimensionality. In what follows, we present a few select examples of open-framework compounds prepared in our laboratory using the hydrothermal method. The compounds, $[Co^{II}(C_{10}H_8N_2)(H_2PO_3)_2]$, **I**, $[C_6N_3H_{20}][Zn_2(AsO_4)(HAsO_4)_2].2H_2O$, **II**, $[NH_3(CH_2)CH(NH_3)CH_3]_3[Fe_6(AsO_4)_2(HAsO_4)_6(C_2O_4)_3]$, **III**, $[C_5N_2H_{14}]$ $[Fe_4(HPO_3)_2(C_2O_4)_3]$, **IV**, $\{Gd(H_2O)_3Co[C_5N_1H_3(COO)_2]_3\}$, **V** and $\{Zn(H_2O)_2[C_5N_1H_3(COO)_2]\}.H_2O$, **VI**, illustrate the efficacy of this method.

2. Experimental

2.1 *Synthesis*

2.1a *$[Co^{II}(C_{10}H_8N_2)(H_2PO_3)_2]$,* **I***:* 0·048 g of Co-powder was dispersed in 3 ml deionised water. To this, 0·272 g of H_3PO_3 and 0·259 g of 4,4′-bipyridine were added and the mixture was stirred at room temperature for 30 min. The final mixture with the composition, 1·0 Co : $4H_3PO_3$: 2(4,4′-bipyridine) : 200 H_2O, was heated at 125°C for 7 days in a 7-ml PTFE-lined acid digestion bomb, to result in large quantities of pink-coloured crystals. The initial pH was ~2 and there was no appreciable change in pH during the reaction.

2.1b *$[C_6H_{20}N_3][Zn_2(AsO_4)(HAsO_4)_2]\cdot 2H_2O$,* **II***:* 0·045 g of ZnO, 0·252 g of As_2O_5, 0·10 ml of acetic acid, and 0·16 ml of 3,3′-diaminodipropyamine (DPTA) were added to a mixture of 1 ml of THF and 2 ml of water The reaction mixture with the composition, 1 ZnO : $2As_2O_5$: 1 CH_3COOH : 2 DPTA : 22 THF : 200 H_2O, was heated at 75°C for 72 h followed by at 150°C for 24 h in a 7-ml PTFE-lined acid-digestion bomb, to result in large quantities of colourless crystals. The initial and final pH values of the reaction mixture were ~4 and ~3 respectively.

2.1c *$[H_3NCH_2CH(NH_3)CH_3]_3[Fe_6^{III}(HAsO_4)_6(AsO_4)_2(C_2O_4)_3]$,* **III***:* 0·297 g of iron(II)oxalate dihydrate was dissolved in 4 ml of millipore water. To this, 1·249 g of H_3AsO_4 and 0·28 ml of 1,2-diaminopropane (1,2-DAP) (99%) were added and the mixture was homogenized for 30 min. at room temperature. The final mixture with the composition, 1·5 $FeC_2O_4\cdot 2H_2O$: 8 H_3AsO_4 : 3 (1,2-DAP) : 200 H_2O, was heated at 150°C for 3 days in a 23-ml PTFE-lined acid-digestion bomb, to result in large quantities of colourless crystals. The initial and final pH of the reaction mixture was ~2 and there was no appreciable change in the pH during the reaction.

2.1d *$[C_5N_2H_{14}][Fe^{II}_4(HPO_3)_2(C_2O_4)_3]$,* **IV***:* 0·177 g of Fe-powder was dispersed in 7 ml of deionised water. To this, 0·521 g of H_3PO_3, 0·400 g of oxalic acid and 0·318 g of homopiperazine were added and the mixture was homogenized for 30 min at room temperature. The final mixture with the composition,

1·0 Fe : 2·0 H_3PO_3 : 1·0 oxalic acid : 1·0 Homopiperazine : 122 H_2O, was heated successfully at 125°C for 96 h, 150°C for 48 h and 180°C for 24 h in a 23-ml teflon-lined acid-digestion bomb to result in mild yellow-coloured crystals. The initial and final pH of the reaction mixture was ~ 2.

2.1e *{$Gd(H_2O)_3Co[C_5N_1H_3(COO)_2]_3$}*, **V***:* 0·343 g of $Gd(NO_3)_3$ and 0·251 g of $Co(OAc)_2{\cdot}4H_2O$ were dissolved in 14 ml deionised water. To this, 0·337 g of pyridine-2,3-dicarboxylic acid (Py-2,3-acid) was added and the mixture was homogenized for 30 min at room temperature. The final mixture with the composition, 1 $Gd(NO_3)_3$: 1 $Co(OAc)_2{\cdot}4H_2O$: 2(Py-2,3-acid) : 780 H_2O, was heated at 140°C for 72 h in a 23-ml PTFE-lined acid-digestion bomb to result in large quantities of pink-coloured crystals.

2.1f *{$Zn(H_2O)_2[C_5N_1H_3(COO)_2]$}$\cdot H_2O$,* ***VI:*** 0·143 g of $ZnSO_4{\cdot}7H_2O$ was dispersed on 3 ml of deionised water. To this, 0·085 g of pyridine-2,5-dicarboxylic acid (Py-2,5-acid), 0·02g of NaOH, 0·079 g of 4,4′-bipyridine and 0·03 ml of triethyl amine (TEA) were added and the mixture was homogenized for 30 min at room temperature. The final mixture with the composition 0·5$ZnSO_4{\cdot}7H_2O$: 0·5 (Py-2,5-acid) : 0·5 NaOH : 0·5 4,4′-Bipy : 0·25 TEA : 170 H_2O was heated at 150°C for 72 h in a 7-ml PTFE-lined acid-digestion bomb to result in large quantities of colourless crystals.

In all the cases, the products were filtered under vacuum and washed thoroughly using deionised water and dried at ambient conditions. In most of the cases, the yield of the solid phase product was ~ 70–80% based on the metal source.

2.2 *Single crystal structure determination*

A suitable single crystal of **I**–**VI** was carefully selected and glued to a thin glass fibre. The single-crystal X-ray diffraction data were collected on a Bruker AXS Smart Apex CCD diffractometer at 293(2) K. The X-ray generator was operated at 50 kV and 35 mA using MoKα (λ = 0·71073 Å) radiation. Data were collected with ω scans of width 0·3°. A total of 606 frames were collected in three different settings of φ (0, 90, 180°) keeping the sample-to-detector distance fixed at 6·03 cm and the detector position (2θ) fixed at –25°. Pertinent experimental details of the structure determination of all the compounds are presented in tables 1 and 2.

The data were reduced using SAINTPLUS,[5] and an empirical absorption correction was applied using the SADABS program.[6] The crystal structure was solved and refined using SHELX-97 present in the WinGx suit of program (version 1.63.04a).[7] The hydrogen atom on the P–H group of compound **I** and **IV** and the hydrogen positions of the amine molecules of **I**–**III** compounds were initially located in the difference Fourier map. Due to the disorder of the amine molecules in **IV**, we have not been able to locate the hydrogen atoms. All the other hydrogen atoms were located in the difference Fourier map and for the final refinement the hydrogen atoms were placed in geometrically ideal positions and refined using the riding mode. The last cycles of refinements included atomic positions, anisotropic thermal parameters for all the non-hydrogen atoms and isotropic thermal parameters for all the hydrogen atoms. Full-matrix-least-squares structure refinement against $|F|^2$ was carried out using the WINGX package of programs.[8]

2.3 *Examples of the use of hydrothermal method*

2.3a *Simple inorganic network structures:* As described above, we have prepared a cobalt phosphite, $[Co^{II}(C_{10}H_8N_2)(H_2PO_3)_2]$, **I**, and a zinc arsenate, $[C_6N_3H_{20}][Zn^{II}{}_2(AsO_4)(HAsO_4)_2]{\cdot}2H_2O$, **II**, possessing open structures. In the structure of **I**, there are two P and one Co atoms in the asymmetric unit that are crystallographically independent. The Co(1) is octahedrally coordinated to four oxygen atoms and two nitrogen atoms of the 4,4′-bipyridine molecule. One of the oxygen atoms, [O(3)], is three-coordinated connecting two Co and a P centre. The Co–O/N bond distances are in the range of 2·052(3) – 2·197(3) Å [av.(Co–O/N) = 2·146 Å] and the O/N–Co–O/N bond angles are in the range of 80·73(11)–175·17(11)° [av. (O/N–Co–O/N) = 106·74°]. The cobalt atom is connected to two distinct phosphorous atoms through Co–O–P bonds. Of the two P atoms, the P(1) atom is connected to the cobalt atom via one P–O–Co bond and possess two terminal P–O linkages, while P(2) is connected by two P–O–Co bonds and possesses one terminal P–O bond. The P–O bond distances are in the range of 1·484(3)–1·550(3) Å [av. (P–O) = 1·521 Å] and the O–P–O bond angles are in the range of 107·61(16)–117·2(15)° [av. (O–P–O) = 111·77°]. The charge-balancing criterion requires the presence of two protons associated with the P–O bonds. Bond valence sum calculations[9] and bond length consideration indicate that P(1)–O(5) with a distance of

Table 1. Crystal data and structure refinement parameters for $[Co^{II}(C_{10}H_8N_2)(H_2PO_3)_2]$, **I**, $[C_6N_3H_{20}][Zn^{II}_2(AsO_4)(HAsO_4)_2]\cdot 2H_2O$, **II** and $[NH_3(CH_2)CH(NH_3)CH_3]_3[Fe_6(AsO_4)_2(HAsO_4)_6(C_2O_4)_3]$, **III**.

Structure parameters	**I**	**II**	**III**
Empirical formula	$CoP_2N_2O_6C_{10}H_{12}$	$Zn_2As_3O_{14}N_2C_6H_{26}$	$C_{15}H_{42}As_8Fe_6N_6O_{44}$
Formula weight	377·093	719·80	1944·96
Crystal system	Monoclinic	Triclinic	Trigonal
Space group	*C*2/*c* (no. 15)	*P*(–1) (no. 2)	*P*-3*c*1 (no. 165)
a (Å)	17·2718(6)	8·5248(2)	13·9899(12)
b (Å)	11·4561(4)	8·76270(10)	13·9899(12)
c (Å)	16·9932(5)	14·08270(10)	14·936(3)
α (°)	90·000	98·5260(10)	90·0
β (°)	119·014(10)	90·7420(10)	90·0
γ (°)	90·000	101·8540(10)	120·0
Volume (Å^3)	2940·4(2)	1017·14(3)	2531·6(5)
Z	8	2	12
T (K)	293(2)	293(2)	2·548
ρ_{calc} (mg m^{-3})	1·704	2·350	6·987
μ (mm^{-1})	1·411	7·271	0·71073
θ range (deg)	2·23 to 23·29°	1·46 to 23·32	1886
λ (MoK$_\alpha$) (Å)	0·71073	0·71073	2·73–27·94
Reflection collected	6037	2936	20858
Unique reflections	2119	1057	2032
Number of parameters	191	271	1835
Goodness of fit (S_{obs})	1·083	0·251	0·0335
R index [$I > 2\sigma(I)$]	R_1 = 0·0423, wR_2 = 0·1189	R_1 = 0·0396, wR_2 = ·0926	R_1 = 0·0323[a]; wR_2 = 0·0914[b]
R (all data)	R_1 = 0·0453, wR_2 = 0·1229	R_1 = 0·0649, wR_2 = 0·1254	R_1 = 0·0365[a]; wR_2 = 0·0938[b]
Largest diff· peak and hole eÅ^{-3}	0·787 and –0·533 eÅ^{-3}	1·043 and –0·788 eÅ^{-3}	1·019 and –1·302

$R_1 = \sum||F_o| - |F_c||/\sum|F_o|$; $wR_2 = \{\sum[w(F_o^2 - F_c^2)]/\sum[w(F_o^2)^2]\}^{1/2}$. $w = 1/[\rho^2(F_o)^2 + (aP)^2 + bP]$
$P = [\max(F_o, O) + 2(F_c)^2]/3$, where a = 0·0580 and b = 7·1718 for **I** and a = 0.0003 and b = 0·0000 for **II** and a = 0·0477 and b = 9·5995 for **III**

1·553(3) Å and P(2)–O(6) with a distance of 1·556(3) Å are protonated. Thus, the phosphite groups are actually H_2PO_3 units. The selected bond distances are presented in table 3.

The structure of **I** consists of a network of CoO_4N_2 octahedra and $H_2P(2)O_3$ units. The Co octahedra share two oxygen atoms, [O(3)], forming an edge-shared dimer, $Co_2O_6N_4$. This dimer units are connected through their vertices with the $H_2P(2)O_3$ units giving rise to four-membered rings, which are connected together forming a one-dimensional ladder-like chain structure (figure 1a). The $H_2P(1)O_3$ units bond with the one-dimensional chains through the three-coordinated oxygen, O(3), atom. To our knowledge, a one-dimensional chain of this type has not been observed before. The one-dimensional ladder-like chains are connected by 4,4′-bipyridine ligands forming a two-dimensional layered structure (figure 1b). The connectivity involving the 4,4′-bipyridine has been known in the literature.[10–12]

The structure of zinc arsenate, $[C_6N_3H_{20}][Zn^{II}_2(AsO_4)(HAsO_4)_2]\cdot 2H_2O$, **II** consists of a network of ZnO_4 and $AsO_3(OH)$ tetrahedral units, linked together giving rise to a two-dimensional structure. The zinc atoms are tetrahedrally coordinated by oxygen atom neighbours with an average Zn–O bond lengths 1·946 Å and O–Zn–O bond angles are in the range 97·0(3)–119·8(3)° [av. O–Zn–O bond angle = 109·3°]. The Zn atoms are connected to the As atoms by Zn–O–As linkages with an average Zn–O–As bond angles of 127·17°. Of the three arsenic atoms, As(2) and As(3) make three As–O–Zn bonds and posses as one terminal linkage, and As(1) makes four As–O–Zn bonds. The As–O distances are in the range 1·651(6)–1·711(6) Å [av. As(1)–O = 1·68 Å] and O–As–O bond angles have an average value of 109·4°. The terminal As(1)–O(4) and As(2)–O(8) bonds with distances of 1·723 and 1·688 Å respectively, are –OH groups. The total negative charge on the framework of –3 is balanced by the presence of one fully protonated

Table 2. Crystal data and structure refinement parameters for $[C_5N_2H_{14}]$ $[Fe^{II}_4(HPO_3)_2(C_2O_4)_3]$, **IV**, $\{Gd(H_2O)_3Co[C_5N_1H_3(COO)_2]_3\}$, **V** and $\{Zn(H_2O)_2[C_5N_1H_3(COO)_2]\}\cdot H_2O$, **VI**.

Structure parameters	**IV**	**V**	**VI**
Empirical formula	$C_{11}H_{16}N_2O_{18}P_2Fe$	$C_{21}H_{15}N_3O_{15}GdCo$	$C_7H_9NO_7Zn$
Formula weight	749·570	765·18	284·52
Crystal system	Monoclinic	Trigonal	Orthorhombic
Space group	$P2(1)/c$ (no. 14)	$P3$ (no. 143)	$P2_12_12_1$ (no. 19)
a (Å)	7·682	13·1879(2)	7·3450(7)
b (Å)	7·726	13·1879(2)	9·4412(10)
c (Å)	18·092	5·9291(10)	13·8459(14)
α (°)	90·000	90·000	90·000
β (°)	94·443(2)	90·000	90·000
γ (°)	90·000	120·000	90·000
Volume (Å^3)	1070·8(3)	893·04(2)	960·15(17)
Z	4	1	4
T (K)	293(2)	293(2)	293(2)
ρ_{calc} (mg m^{-3})	2·004	1·412	1·968
μ (mm^{-1})	1·589	2·363	2·580
θ range (deg)	2·26 to 27·99	1·78 to 23·32	2·61 to 20·81
λ (MoK$_\alpha$) (Å)	0·71073	0·71073	0·71073
Reflection collected	8974	3745	4672
Unique reflections	2538	1689	1005
Number of parameters	172	126	153
Goodness of fit (Sobs)	1·053	1·142	1·107
R index [I > 2σ(I)]	R_1 = 0·0376, wR_2 = 0·0993	R_1 = 0·0378, wR_2 = 0·1050	R_1 = 0·0132,[a] wR_2 = 0·0361[b]
R (all data)	R_1 = 0·0394, wR_2 = 0·1006	R_1 = 0·0402, wR_2 = 0·1067	R_1 = 0·0132, wR_2 = 0·0362
Largest diff· peak and hole eÅ^{-3}	1·740 and –0·892	0·963 and –0·756	0·364 and –0·166

$R_1 = \Sigma||F_o| - |F_c||/\Sigma|F_o|$; $wR_2 = \{\Sigma[w(F_o^2 - F_c^2)]/\Sigma[w(F_o^2)^2]\}^{1/2}$. $w = 1/[\rho^2(F_o)^2 + (aP)^2 + bP]$
$P = [\max(F_o, O) + 2(F_c)^2]/3$, where a = 0·0551 and b = 2·8935 for **IV**; a = 0·0597 and b = 0·000 for **V**; and a = 0·0248 and b = 0·000 for **VI**

3,3′-diaminodipropylamine (DPTA) molecule. Selected bond distances are listed in table 3.

The structure is formed by strictly alternating ZnO_4 and $AsO_3(OH)$ tetrahedral units, connected through their vertices forming one-dimensional ladder-like structure. The one-dimensional ladders are further bonded through the four-membered rings giving rise to a layer structure with apertures bound by 8-T atoms (T = Zn, As). The tetrahedral $AsO_3(OH)$ groups, which are bonded to the Zn atom, hang from the layer and protrude into the inter-lamellar region within which the protonated amine molecules also reside (figure 2). Similar structural arrangements have been observed in open-framework zinc phosphate structures.[13] The protonated organic amine molecules along with the lattice water molecules are located in the inter-lamellar region as shown in figure 3. Multipoint hydrogen bonding is important in low-dimensional solids for the structural stability. Since the compounds contains pendant As–OH and As = O bonds, they can participate in hydrogen-bond interactions. Large number of hydrogen bonds involving organic amine, lattice water and framework oxygen atoms have been observed in **II**.

2.3b *Inorganic-organic hybrid network structures:* As part of our continuing search for new materials with novel structures, we have also prepared compounds containing two different anions, one derived purely from an inorganic source and the other from organic. Thus, we have compounds containing oxalate units as part of the network along with phosphite and arsenate anions. The structure of the iron oxalate-arsenate, $[NH_3(CH_2)CH(NH_3)CH_3]_3[Fe_6(AsO_4)_2(HAsO_4)_6(C_2O_4)_3]$, **III**, consists of a network of FeO_6 octahedral, AsO_4 tetrahedral and C_2O_4 units linked together giving rise to a three-dimensional structure. The Fe atoms are coordinated to six oxygen atom neighbours with four short and two longer Fe–O distances. The Fe–O distances are in the range 1·929(3)–2·145(3) Å (av. 2·018 Å), the shorter distances corresponding to the Fe–O–As and the longer

Table 3. Selected bond distances in $[Co^{II}(C_{10}H_8N_2)\ (H_2PO_3)_2]$, **I**, $[C_6N_3H_{20}]$ $[Zn_2(AsO_4)(HAsO_4)_2]\cdot 2H_2O$, **II**, $[NH_3(CH_2)CH(NH_3)CH_3]_3[Fe_6(AsO_4)_2(HAsO_4)_6(C_2O_4)_3]$, **III**, $[C_5N_2H_{14}]$ $[Fe_4(HPO_3)_2(C_2O_4)_3]$, **IV**, $\{Gd(H_2O)_3\,Co[C_5N_1H_3(COO)_2]_3\}$, **V** and $\{Zn(H_2O)_2$ $[C_5N_1H_3(COO)_2]\}\cdot H_2O$, **VI**.

*Compound **I***			
Co(1)–O(1)	2·052(3)	P(1)–O(4)	1·484(3)
Co(1)–O(3)$^{\#1}$	2·158(3)	P(1)–O(5)	1·553(3)
Co(1)–O(2)	2·112(3)	P(1)–O(3)	1·532(3)
Co(1)–O(3)	2·176(3)	P(2)–O(1)$^{\#2}$	1·493(3)
Co(1)–N(1)	2·181(3)	P(2)–O(2)	1·513(3)
Co(1)–N(2)	2·197(3)	P(2)–O(6)	1·556(3)
*Compound **II***			
As(1)–O(1)	1·653(6)	As(3)–O(11)	1·688(6)
As(1)–O(2)	1·668(6)	As(3)–O(12)	1·683(6)
As(1)–O(3)	1·677(6)	Zn(1)–O(5)$^{\#3}$	1·975(6)
As(1)–O(4)	1·723(6)	Zn(1)–O(6)$^{\#1}$	1·929(6)
As(2)–O(5)	1·666(6)	Zn(1)–O(9)	1·965(6)
As(2)–O(6)	1·671(6)	Zn(1)–O(11)$^{\#2}$	1·942(6)
As(2)–O(7)	1·687(6)	Zn(2)–O(2)	1·949(6)
As(2)–O(8)	1·688(6)	Zn(2)–O(7)	1·925(6)
As(3)–O(9)	1·676(6)	Zn(2)–O(10)	1·952(6)
As(3)–O(10)	1·674(6)	Zn(2)–O(12)$^{\#4}$	1·930(6)
*Compound **III***			
As(1)–O(1)	1·664(3)	Fe(1)–O(1)	1·929(3)
As(1)–O(2)	1·668(3)	Fe(1)–O(5)	1·951(3)
As(1)–O(3)	1·678(3)	Fe(1)–O(3)$^{\#2}$	1·951(3)
As(1)–O(4)	1·717(3)	Fe(1)–O(2)$^{\#3}$	1·994(3)
As(2)–O(5)$^{\#1}$	1·673(3)	Fe(1)–O(7)	2·133(3)
As(2)–O(5)	1·673(3)	Fe(1)–O(8)	2·145(3)
As(2)–O(5)$^{\#2}$	1·673(3)	C(1)–O(7)$^{\#4}$	1·256(3)
As(2)–0(6)	1·715(4)	C(2)–O(8)$^{\#4}$	1·253(4)
		C(1)–C(2)	1·536(7)
*Compound **IV***			
Fe(1)–O(1)	1·994(2)	Fe(2)–O(8)$^{\#2}$	2·100(2)
Fe(1)–O(2)	2·088(2)	Fe(2)–O(4)	2·105(2)
Fe(1)–O(3)	2·106(2)	Fe(2)–O(9)$^{\#2}$	2·153(2)
Fe(1)–O(4)	2·118(2)	Fe(2)–O(3)	2·239(2)
Fe(1)–O(5)	2·220(2)	P(1)–O(7)	1·508(2)
Fe(1)–O(6)	2·260(2)	P(1)–O(1)	1·521(2)
Fe(2)–O(7)#1	1·980(2)	P(1)–O(4)$^{\#3}$	1·531(2)
*Compound **V***			
Gd(1)–O(1)$^{\#1}$	2·406(7)	Gd(1)–O(3)$^{\#1}$	2·504(6)
Gd(1)–O(1)	2·406(7)	Co(1)–O(4)	1·884(6)
Gd(1)–O(1)$^{\#2}$	2·406(7)	Co(1)–O(4)$^{\#3}$	1·884(6)
Gd(1)–O(2)$^{\#2}$	2·450(6)	Co(2)–O(4)$^{\#4}$	1·884(6)
Gd(1)–O(2)	2·450(6)	Co(1)–N(1)$^{\#3}$	1·992(7)
Gd(1)–O(2)$^{\#1}$	2·450(6)	Co(1)–N(1)	1·992(7)
Gd(1)–O(3)$^{\#2}$	2·504(6)	Co(1)–N(1)$^{\#4}$	1·992(7)
Gd(1)–O(3)	2·504(6)		
*Compound **VI***			
Zn(1)–O(1)	2·050(3)	Zn(1)–O(4)	2·120(3)
Zn(1)–O(2)	2·054(3)	Zn(1)–N(1)	2·136(3)
Zn(1)–O(3)	2·075(3)	Zn(1)–O(5)	2·278(3)

Symmetry transformations used to generate equivalent atoms: #1 $-x+1, y, -z+1/2$; #2 $-x+1, -y+1, z$; #3 $x, y-1, z$; #4 $x, y+1, z$ for **I**, #1 $x-1, y, z$; #2 $-x, -y+1, -z+2$; #3 $-x+1, -y+2, -z+2$; #4 $-x+1, -y+1, -z+2$; #5 $x+1, y, z$ for **II**, #1 $-y+1, x-y+1, z$; #2 $-x+y, -x+1, z$; #3 $-x+1, -y+2, -z+1$; #4 $x-y+1, -y+2, -z+3/2$ for **III** #1 $x, y-1, z$; #2 $x-1, y, z$; #3 $-x, y+1/2, -z+1/2$ for **IV**, #1 $-x+y+1, -x+1, z$; #2 $-y+1, x-y, z$; #3 $-x+y, -x, z$; #4 $-y, x-y, z$ for **V**

distances corresponding to the Fe–O–C linkages; these distances are consistent with the iron being in the 3+ oxidation state. The O–Fe–O bond angles are in the range 87·05(11) –174·35(12)°. While all the FeO_6 vertices are shared with either the As or C atoms through the oxygen linkages, only three of the vertices of the AsO_4 units are shared, the remaining ones being either As = O or As–OH bonds. The As atoms have tetrahedral coordination with As–O distances in the range 1·664(3)–1·717(3) Å [av. 1·685 Å for As(1) and 1·682 Å for As(2), respectively]. The O–As–O bond angles are in the range 105·09(9)–114·80(14)° (av. 109·3°). The C–O bond distances and O–C–O bond angles are in the range expected for this type of bonding. Selected bond distances are given in table 3.

The framework consists of FeO_6, AsO_4, $HAsO_4$ and C_2O_4 moieties. Connectivity between the FeO_6, AsO_4 and $HAsO_4$ polyhedral units leads to an inorganic layer of formula $[Fe_3(HAsO_4)_3(AsO_4)]$, with the FeO_6 and AsO_4 tetrahedra strictly alternating within the layer. The layers are porous, encompassing a circular 12-membered ring as shown in figure 4; this layer is topologically identical to that seen in the porous aluminophosphate based upon the $Al_3P_4O_{16}^{3-}$ ion, with which it shares the same space group, $P\text{-}3c_1$[14] (note that other layered aluminum phosphates with the $Al_3P_4O_{16}^{3-}$ stoichiometry are based entirely on tetrahedral nets).[15] The architecture of **III** has also been seen in an iron oxalatophosphate.[16] The 12-membered pores within the layers are surrounded by 4-membered rings, of which there are two distinct types. In one set of these rings, the arsenic atoms are part of the wall of the 12-membered ring, while in the other an arsenate group caps a six-membered ring and alternates above and below the plane of the inorganic layers (figure 4). The layers are arranged in *AAAA*… fashion and are held in place by oxalate pillars. The

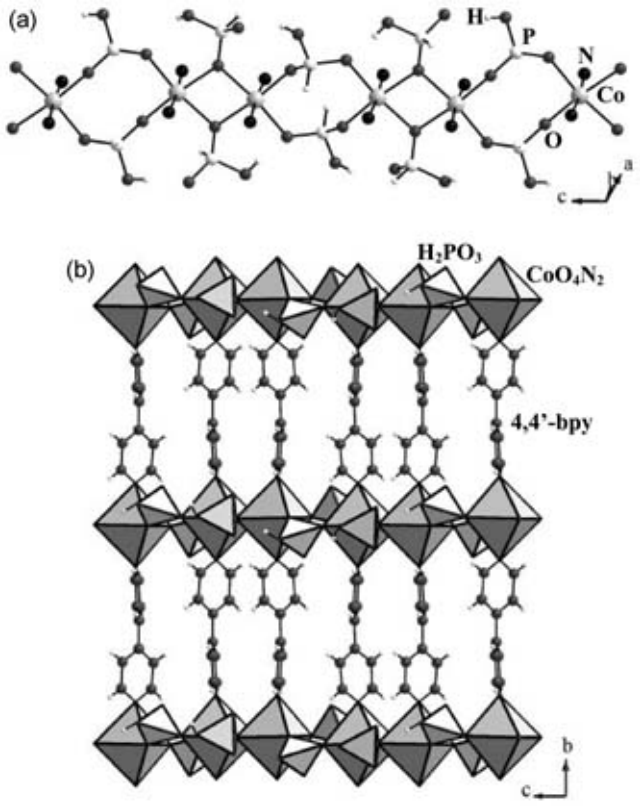

Figure 1. (**a**) Structure of **I**, showing the one-dimensional ladder-like chains. Note that the H_2PO_3 group hangs from the three-coordinated oxygen atoms of the chain. (**b**) Figure shows the connectivity between the one-dimensional chains and 4,4′-bipyridine units giving rise to a two-dimensional layer.

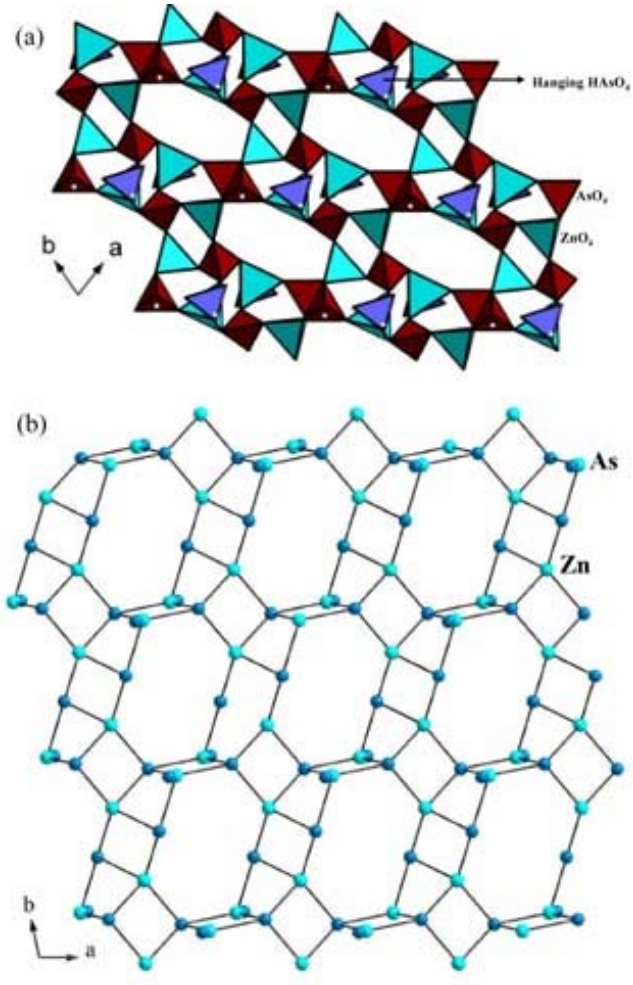

Figure 2. (**a**) Polyhedral view of the structure of **II** in the *ab* plane. Note the presence of the hanging arsenate groups. (**b**) Figure shows the T-atom (T = Zn, P) connectivity within the layer.

oxalate units are coordinated to the iron centres and connect the adjacent layers (figure 5).

The negative charge of the framework of the iron oxalatoarsenate, **III**, is compensated by the 1,2-diammoniumpropane cations. Within the structure of **III**, the porous layers are arranged exactly one over the other, giving rise to a supermesh of apertures. The organic amine molecules, which are disordered in **III**, occupy the one-dimensional channels that are oriented perpendicular to the inorganic sheets. This results in completely filled channels and no adsorption behaviour was observed. While the structure of **III** is closely related to that of the iron oxalatophosphate, $[NH_3(CH_2)_2NH_3]_3[Fe_6(PO_4)_2(HPO_4)_6(C_2O_4)_3]\cdot H_2O$ (x = 3–4), reported earlier,[16] the 1,2-diaminopropane in **III** is replaced by ethylenediamine and labile water. The replacement of larger amines by smaller ones plus water has been observed in other systems, such as open framework gallium phosphates.[17]

The asymmetric unit of **IV** contains 19 non-hydrogen atoms of which two Fe and one P atoms are crystallographically independent. The Fe(1) atoms are octahedrally coordinated with respect to oxygen atoms with average distances of 2·131 and 2·115 Å respectively. The O–Fe–O bond angle are in the range 76·48(9)–166·92(9)°. The iron atoms are connected to a phosphorous atom through Fe–O–P bonds and to oxalate groups through Fe–O–C bonds with average bond angle of 130·42 and 118·16° respectively. The iron atoms are also connected to each other through three-coordinated oxygen atoms [O(3) and O(4)] with average Fe–O–Fe bond angle of 101·07°. The P atoms are connected to the iron atom via three Fe–O–P bond and possess one terminal P–H bond. The P–O bond distances are in the range of 1·503(2)–1·531(3) Å [av. (P–O) = 1·520 Å] and the O–P–O bond angles are in the range of 110·60(13)–112·88(14)° [av. (O–P–O) = 111·61°].

The structure of **IV** is built up from a linkage involving the FeO_6 octahedra, the HPO_3 pseudotetrahedra and the oxalate units. The iron atoms are connected to each other through two three-coordinated oxygen atoms [O(3) and O(4)] forming a edge-shared dimer, Fe_2O_{10}, and the dimers are linked through their corners, involving another three-coordinate oxygen atom [O(6)], giving rise to infinite one-dimensional helical chains of Fe–O–Fe (figure 6a). The phosphite units are grafted to these chains forming a one-dimensional structure as shown in figure 6b. The oxalate moieties bond with the iron centre through *in-plane* connectivity forming a hybrid layer and by *out-of-plane* connectivity with the layer to form the

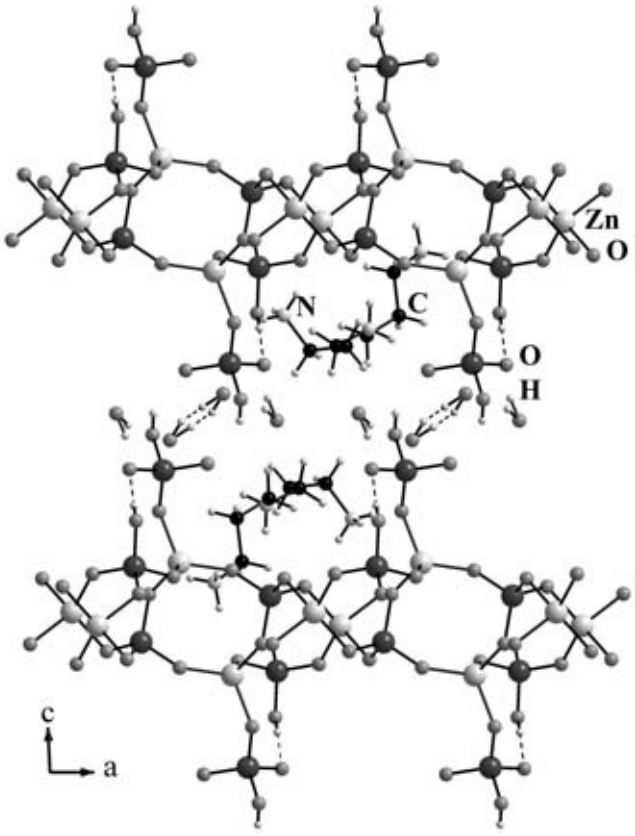

Figure 3. Structure of **II** in the *ac* plane showing the arrangement of the layers. Dotted lines represent the possible hydrogen bond interactions.

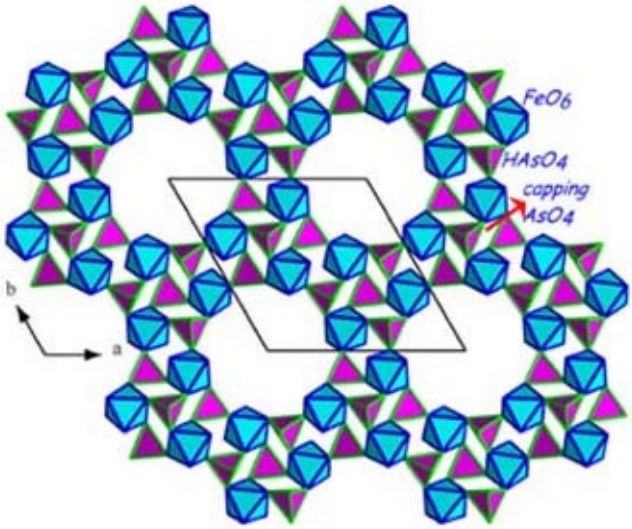

Figure 4. Structure of **III** in the *ab* plane showing the 12-membered pore-opening. The amine molecules and the oxalate units are not shown for clarity.

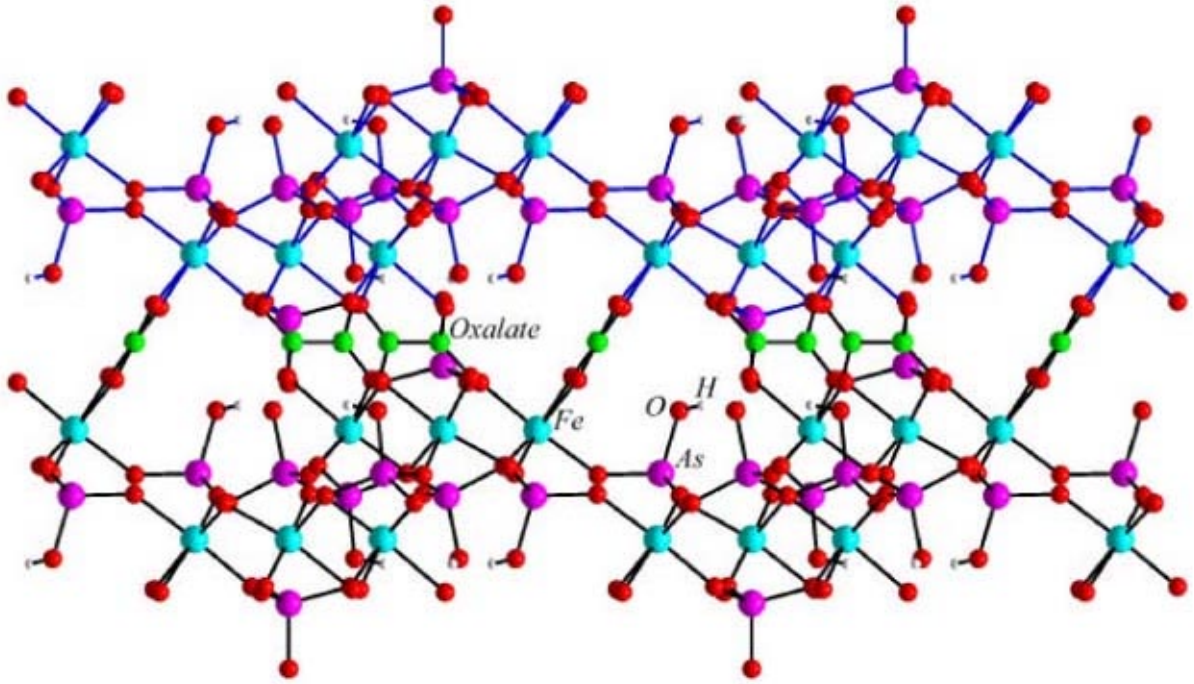

Figure 5. Structure of **III** viewed perpendicular to the inorganic layers, showing the connectivity between these layers by the oxalate groups.

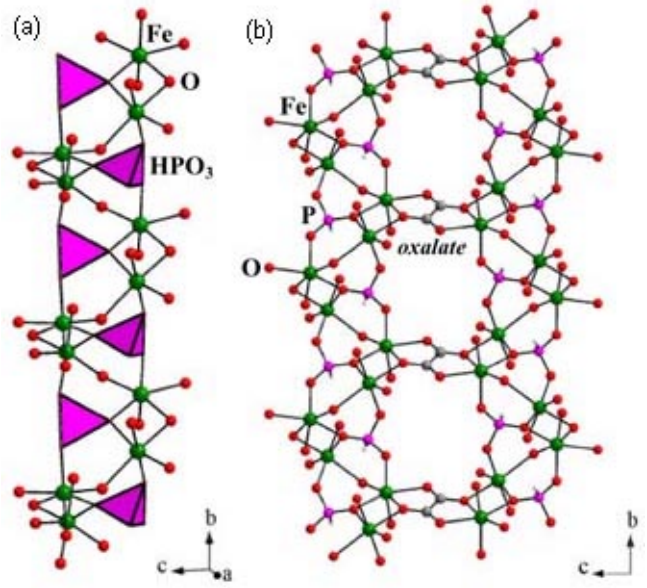

Figure 6. (**a**) The one-dimensional Fe–O–Fe chain in **IV**. (**b**) The one-dimensional structure formed by the linkage between iron and phosphite units. Oxalate units are not shown for clarity.

three-dimensional structure with channels (figure 7). Similar connectivity has been observed before in oxalatephosphite[18] and oxalatophosphate structures.[19] The organic amine molecule occupy the middle of the channels formed by this connectivity.

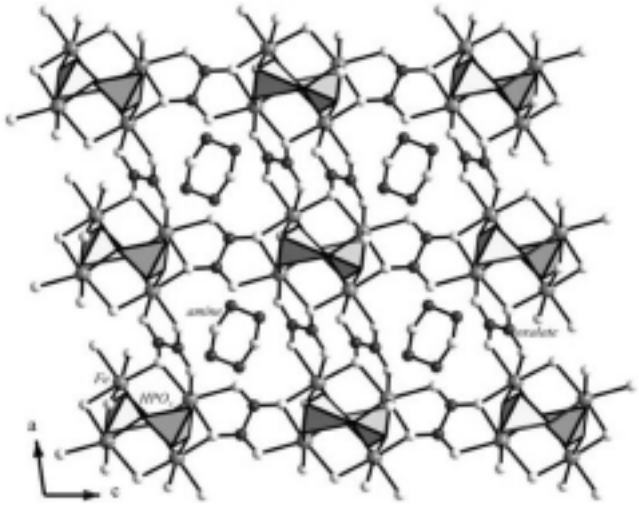

Figure 7. The connectivity between Fe and oxalate units forming the iron oxalate three-dimensional structure. The piperazine molecules occupy the channels.

From the structural point of view, the structure of **IV** presents many unique features. The first and foremost is the presence of infinite one-dimensional helical Fe–O–Fe chains. Though infinite Fe–O–Fe chains have been observed before in ironphosphates,[20] such a structural feature has not been commonly observed in inorganic–organic hybrid structures. Secondly, the connectivity between the phosphite

units and Fe–O–Fe chains give rise to a one-dimensional tancoite-like structure. Tancoite structure has the general formula, $[M(TO_4)_2\varphi]_n$ (M is an octahedrally coordinated element, T is a tetrahedrally coordinated element and φ is an anionic ligand; e.g. O^{2-}, OH^-, F^- etc.). It has been observed that the one-dimensional iron phosphates, in general, form with the tancoite structure.[21]

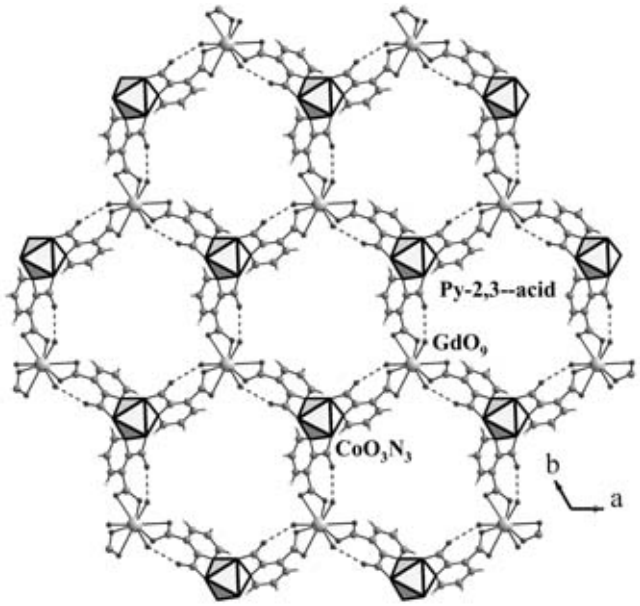

Figure 8. View of the structure of **V** in the *ab* plane showing a single layer. Dotted lines represent possible hydrogen bond interaction. Note that the hydrogen bond interaction creates specific pockets of hybrophilicity within the aperture.

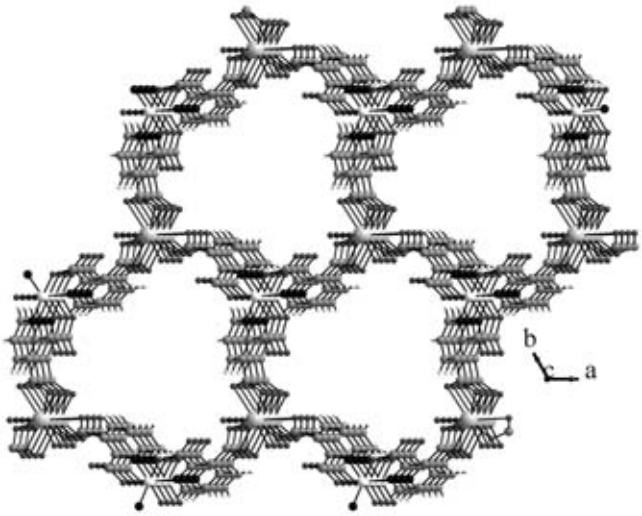

Figure 9. View of the structure of **V** showing the arrangement of the layers. Note that the layers are arranged in a *AAAA* … fashion giving rise to a one-dimensional channel.

2.3c *Coordination polymer structures:* We have prepared mixed metal (3*d*–4*f*) coordination polymer of the formula, $\{Gd(H_2O)_3Co[C_5N_1H_3(COO)_2]_3\}$, **V**. The asymmetric unit of **V** consists 15 non-hydrogen atoms, of which one gadolinium atom and one cobalt atom are crystallographically independent. The Gd^{+3} and the Co^{+3} are located in special positions with a site occupancy of 0·33, respectively (Gd^{+3} occupies the *1c* site and Co^{+3} occupies the *1a* site). Gd^{+3} ions are bonded with nine nearest neighbour oxygen atoms and have a tricapped trigonal prismatic geometry. Of the nine oxygen atoms, three oxygen atoms belong to the terminal water molecules and six to the carboxylate oxygen atoms. The Co^{+3} ions have an octahedral geometry formed by three carboxylate oxygen atoms and three nitrogen atoms of the pyridine ring. The average distances of 2·45 Å for the Gd–O and 1·88 Å and 1·99 Å for the Co–O and Co–N bonds respectively, result from this connectivity. The O–Gd–O bond angles are in the range 52·7(2)–149·0(3)° and the O/N–Co–O/N bond angles are in the range 84·5(3)–173·8(3)°. The selected bond distances are listed in table 3. There is only one type of pyridine-2,3-dicarboxylate anion present in the structure.

The two carboxylate units of the pyridine-2,3-dicarboxylate show differences in the connectivity with respect to the Gd^{+3} and Co^{+3} ions – one having a monodentate connectivity with the Co^{+3} ions and

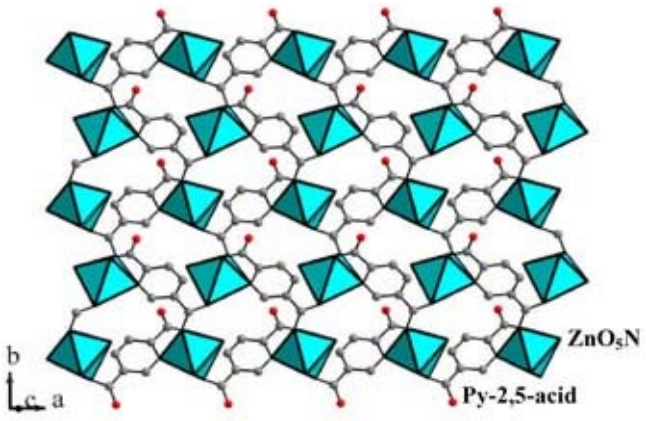

Figure 10. View of the structure of **VI** in the *ab* plane showing a single layer.

the other a *bis*-bidentate connectivity with the Gd^{+3} ions. The nitrogen atom of the pyridine ring is bonded only with the Co^{+3} ions. The connectivity between the polyhedral units and the pyridine carboxylate anions give rise to a two-dimensional neutral layered structure with large apertures bound by 12-membered ring ($3GdO_9$, $3CoO_3N_3$ and six pyridine dicarboxylate) (figure 8). The layers are arranged in *AAAA*… fashion, giving rise to a solid with a supermesh of apertures of ~ 7 Å free diameter (figure 9). The water molecules, bound to Gd, take part in strong hydrogen bond interactions with the neighbouring non-bonded terminal oxygen atom of the carboxylate (O … O distance = 2·85 Å). Such is the disposition of the water molecules within the apertures that there are specific pockets within the apertures (channels) that are hydrophilic.

The asymmetric unit of zinc pyridine-2,5-dicarboxylate, $\{Zn(H_2O)_2[C_5N_1H_3(COO)_2]\}\cdot H_2O$, **VI**, contains 16 non-hydrogen atoms, of which one zinc atom is crystallographically independent. The Zn^{+2} ions have an octahedral geometry formed by three carboxyalate oxygen atoms, one nitrogen atom of pyridine ring and two oxygen atom of the terminal water molecules. The average distances of 2·115 Å for the Zn–O and 2·136 Å for the Zn–N bonds, result from this connectivity. The O/N–Zn–O/N bond angles are in the range 77·8(12)–173·21(10)°. The selected bond distances are listed in table 2.

There is only one type of pyridine-2,5-dicarboxylate anion present in the structure. The two carboxylate units of the pyridine-2,5-dicarboxylate show differences in their connectivity with respect to the Zn^{+2} ions. Thus, the carboxylate group that is the nearest to the nitrogen atom of the pyridine ring has a monodentate connectivity while the other carboxylate group has a *bis*-bidentate connectivity with the Zn^{+2} ions. The connectivity between the ZnO_5N octahedra and the pyridine carboxylate anions gives rise to a two-dimensional neutral layer structure as shown in figure 10.

3. Concluding remarks

The use of hydrothermal methods over the past years has enabled the discovered of many novel materials possessing channels and other features of potential technological applications. It is significant that one is in a somewhat better position today to design these structures based on the understanding of the processes involved in their formation. We are, however, far from being able rationally to design materials with the desired dimensionality or porosity. There is still much to be done to unravel fully the role of the amine and the process(s) involved in the assembly of complex three-dimensional structures from simpler units. One feature that has become apparent is that the formation of open-framework structures is not slow and step-wise throughout, but is likely to involve the spontaneous assembly of preformed units. There is still considerable scope to explore newer structures possessing novel properties such as ferromagnetic channels. It would be of great value if one can find ways to remove the amines present in the channels or between the layers in the open-framework structures. These are some of the challenges at present, but it is clear that the use of hydrothermal technique for the preparation of inorganic compounds continues to be interesting.

Acknowledgments

SN thanks the Department of Science and Technology, Government of India for the award of a research grant. The authors also thank DST–IRHPA for the CCD facility.

References

1. Barrer R M 1948 *J. Chem. Soc*. 2158
2. Barrer R M 1982 *Hydrothermal chemistry of zeolites* (London: Academic Press)
3. Rao C N R, Natarajan S and Vaidhyanathan R 2004 *Angew. Chem. Int. Ed.* **42** 1426
4. Cheetham A K, Loiseau T and Ferey G 1999 *Angew. Chem. Int. Ed.* **38** 3268
5. SMART (V 5.628), SAINT (V 6.45a), XPREP, SHELXTL, Bruker AXS Inc. Madison, Wisconsin, USA, 2004
6. Sheldrick G M 1994 *Siemens area correction absorption correction program.* University of Göttingen, Göttingen, Germany
7. Sheldrick G M 1997 *SHELXL-97 program for crystal structure solution and refinement*, University of Göttingen, Göttingen, Germany
8. Farrugia J L 1999 *J. Appl. Crystallogr.* **32** 837
9. Brown I D and Altermatt D 1985 *Acta Crystallogr.* **B41** 244
10. Chang W-K, Chiang R-K, Jiang Y-C, Wang S-L, Lee S-F and Lii K-H 2004 *Inorg. Chem.* **43** 2564
11. Huang C-H, Huang L-H, Lii K-H 2001 *Inorg. Chem.* **40** 2625
12. Huang L-H, Kao H-M and Lii K-H 2002 *Inorg. Chem.* **41** 2936
13. Natarajan S 2002 *Chem. Commun*. 780

14. Thomas J M, Jones R H, Xu R, Chen J, Chippindale A M, Natarajan S and Cheetham A K 1992 *J. Chem. Soc., Chem. Commun.* 929
15. Jones R H, Thomas J M, Xu R, Huo Q, Cheetham A K and Powell A V 1991 *J. Chem. Soc., Chem. Commun.* 1266
16. Choudhury A, Natarajan S and Rao C N R 1999 *Chem. Mater.* **11** 2316
17. Férey G 1995 *J. Fluorine Chem.* **72** 187
18. Mandal S, Pati S K, Green M A and Natarajan S 2005 *Chem. Mater.* **17** 2912
19. Choudhury A, Natarajan S and Rao C N R 1999 *J. Solid State Chem.* **146** 538
20. Choudhury A, Natarajan S and Rao C N R 1999 *Chem. Commun.* 1305
21. Cavellec M, Riou D, Greneche J-M and Ferey G 1997 *Inorg. Chem.* **36** 2187